

Analysis of Earthquake-Triggered Failure Mechanisms of Slopes and Sliding Surfaces

WANG Jian^{1*}, YAO Lingkan^{1,2,3}, Arshad Hussain⁴

¹ School of Civil Engineering, Southwest Jiaotong University, Chengdu 610031, China

² MOE Key Laboratory of High-speed Railway Engineering, Southwest Jiaotong University, Chengdu 610031, China

³ Road and Railway Engineering Research Institute, Sichuan Key Laboratory of Aseismic Engineering and Technology, Chengdu 610031, China

⁴ National University of Sciences and Technology (NUST), Islamabad 44000, Pakistan

* Corresponding author, E-mail: crest01@qq.com; Tel: + 86 (028)87634192

© Science Press and Institute of Mountain Hazards and Environment, CAS and Springer-Verlag Berlin Heidelberg 2010

Abstract: Earthquake-induced landslides along the Dujiangyan-Yingxiu highway after the Ms 8.0 Wenchuan earthquake in 2008 were investigated. It was found that: (1) slopes were shattered and damaged during the earthquake and open tension cracks formed on the tops of the slopes; (2) the upper parts of slopes collapsed and slid, while the lower parts remained basically intact, indicating that the upper parts of slopes would be damaged more heavily than the lower parts during an earthquake.

Large-scale shaking table model tests were conducted to study failure behavior of slopes under the Wenchuan seismic wave, which reproduced the process of deformation and failure of slopes. Tension cracks emerged at the top and upper part of model, while the bottom of the model remained intact, consistent with field investigations. Depth of the tension crack at the top of model is 32 cm, i.e., 3.2 m compared to the prototype natural slope with a height of 14 m when the length scale ratio (proto/model) is 10. Acceleration at the top of the slope was almost twice as large as that at the toe when the measured accelerations on shaking table are 4.85 m/s² and 6.49 m/s², which means that seismic force at the top of the slope is twice the magnitude of that at the toe.

By use of the dynamic-strength-reduction method, numerical simulation was conducted to explore the process and mechanism of formation of the sliding surface, with other quantified information. The earthquake-induced failure surfaces commonly consist of tension cracks and shear zones. Within 5 m

from the top of the slope, the dynamic sliding surface will be about 1 m shallower than the pseudo-static sliding surface in a horizontal direction when the peak ground acceleration (PGA) is 1 m/s²; the dynamic sliding surface will be about 2 m deeper than the pseudo-static sliding surface in a horizontal direction when the PGA is 10 m/s², and the depths of the dynamic sliding surface and the pseudo-static sliding surface will be almost the same when the PGA is 2 m/s².

Based on these findings, it is suggested that the key point of anti-seismic design, as well as for mitigation of post-earthquake, secondary mountain hazards, is to prevent tension cracks from forming in the upper part of the slope. Therefore, the depth of tension cracks in slope surfaces is the key to reinforcement of slopes. The depth of the sliding surface from the pseudo-static method can be a reference for slope reinforcement mitigation.

Key words: Subgrade engineering; slope failure mechanism; shaking table model test; seismic sliding surface; Wenchuan earthquake

Introduction

Failure mechanisms of slopes during earthquakes have become the focus of studies dealing with the complexity of geotechnical earthquake engineering at the present. Failure mechanisms of slopes under static stations are still employed to analyze their stability during

Received: 7 January 2010
Accepted: 1 May 2010

earthquakes, which interprets the failure of slope under dynamic stations as caused by shearing, and it is applied as the basis for calculation of slope stability (Crespellanit et al. 1998; Wright et al. 2004; Havenith et al. 2003; CHEN et al. 2004; Baker et al. 2006). In the field investigations of the Wenchuan earthquake effects, it was found that tops of the slopes were intensely cracked by the earthquake (HUANG et al. 2009; WANG et al. 2009; LI et al. 2009; CUI et al. 2009a; CUI et al. 2009b). The critical need is to analyze in detail the landsliding processes during an earthquake, learning the stress patterns, failure mechanisms and the nature of the failed slope surfaces.

This paper presents a study on seismically induced landslides observed along the Dujiangyan-Yingxiu highway. Firstly, a field investigation was conducted to determine the characteristics of the coseismic landslides. Later, large-scale shaking table model tests were performed to find how seismic activity affected slopes and what makes seismic landslides unique. Finally, the dynamic-strength-reduction method was used to numerically analyze the failure mechanism of slopes, and to analyze the depth of the sliding surface quantitatively. These findings can be the reference and basis for pre-earthquake anti-seismic design and post-earthquake mitigation.

1 Field Investigations

A typical coseismic landslide is located at Baishuixi Bridge approaching Yingxiu, a location with earthquake intensity IX. The location of top of the slope is $31^{\circ}00.875\text{N}$, $103^{\circ}32.833\text{E}$ (see Figure 1).

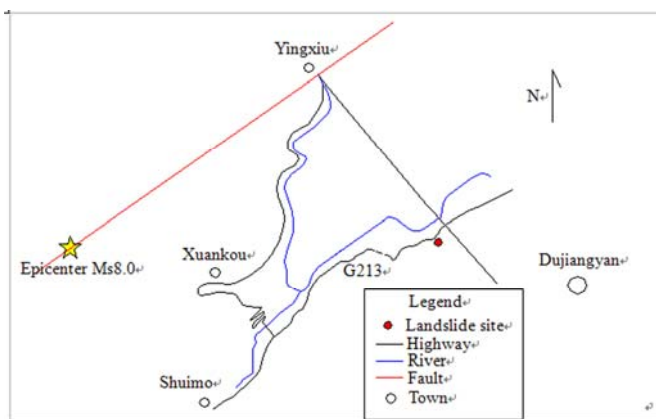


Figure 1 Location of field investigations

The site slopes at an angle of 34.5° towards the north. Height of the slope is 90 m, and the length is 51 m. The collapsed volume is about 50,000 cubic meters (see Figure 2). The slope was shattered and damaged during the earthquake and open tension cracks were formed at the top of the slope with a width of 40 cm and a length of more than 1 m (see Figure 2a). The upper part of slope (here named the collapsing-sliding area) collapsed and slid, while the lower part of the slope remained intact basically (here named the intact area), which indicated that the upper part of the slope would be damaged more heavily than the lower part during an earthquake. The area covered with block and talus deposits at the base of the slope is here called the accumulating area (see Figure 2b).

The engineering-geological section of the landslide is shown in Figure 2c. The formations in the descending order are: (1) colluvium of the Quaternary Period (Q_4^{c+dl}): light-yellow and yellow earth-rock aggregate, spread all over the surface of the slope, with a depth of about 10m. (2) Jurassic-age (JWC¹): rock composed of conglomerate (60%-70%), quartzite (38%), sandstone (20%-30%) and a little flint, with a depth of about 30 m. Diameter of the gravel clasts is often between 2 and 8 cm, with largest one up to 30 cm. (3) Triassic-age (T_{3xj}): grey to dark grey sandstone and grey to grey-black carbonaceous shale, with outcrops of more than 100 m. The collapsed sliding mass is mainly made up of colluvium and conglomerate.

2 Large-Scale Shaking Table Model Tests

To study the failure mechanism of slopes during an earthquake, shaking table model tests were performed on the shaking table of the Road and Railway Engineering department, Southwest Jiaotong University in Chengdu. The system has a payload capacity of 25 tons and can be used for large-scale model tests. A total number of 6 accelerometer sensors were used for measurements during the test. A layout of the instruments is shown in Figure 3.

2.1 Model design

The soil used in this study is colluvium composed of earth-rock aggregate and is classified as well graded gravel (GW). The soil sample was

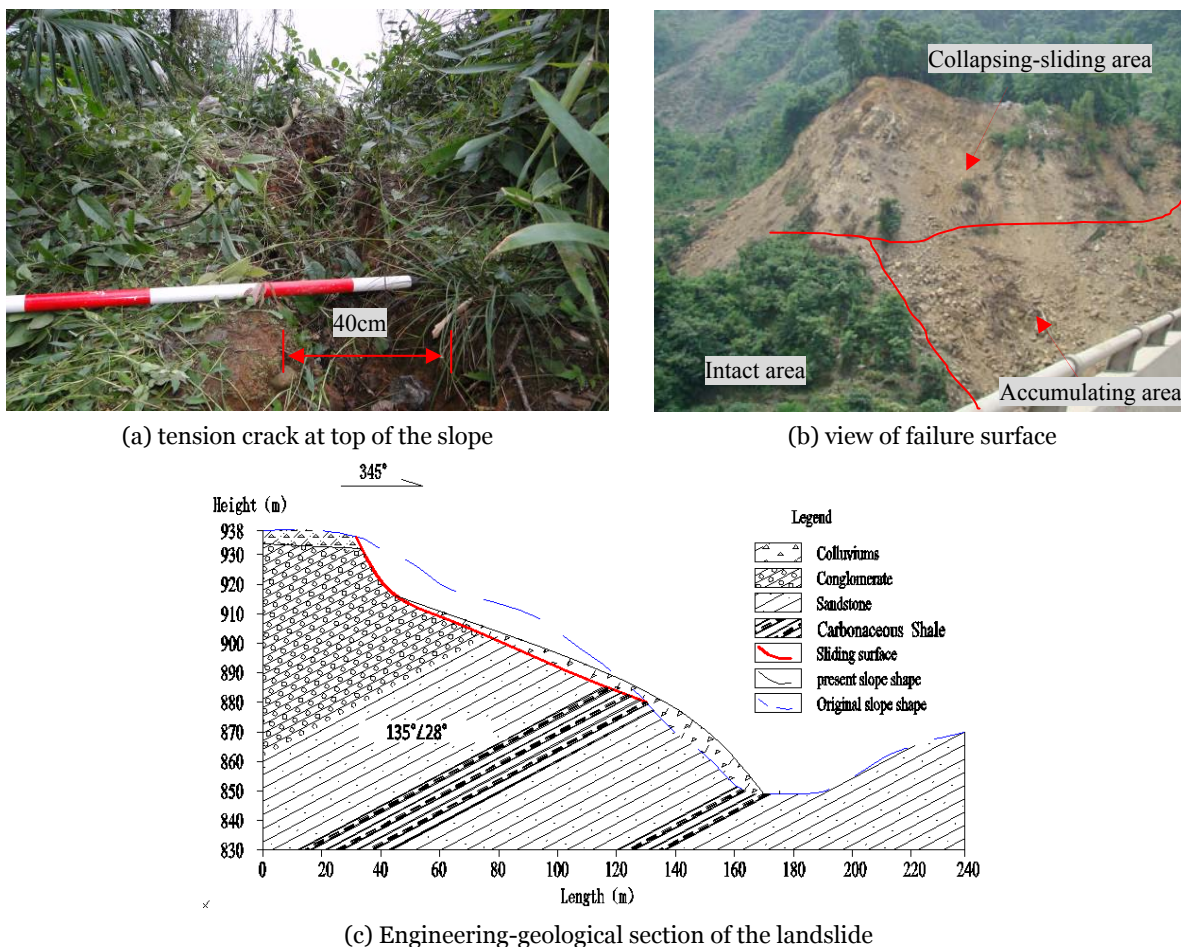


Figure 2 Landslide triggered by the Wenchuan earthquake

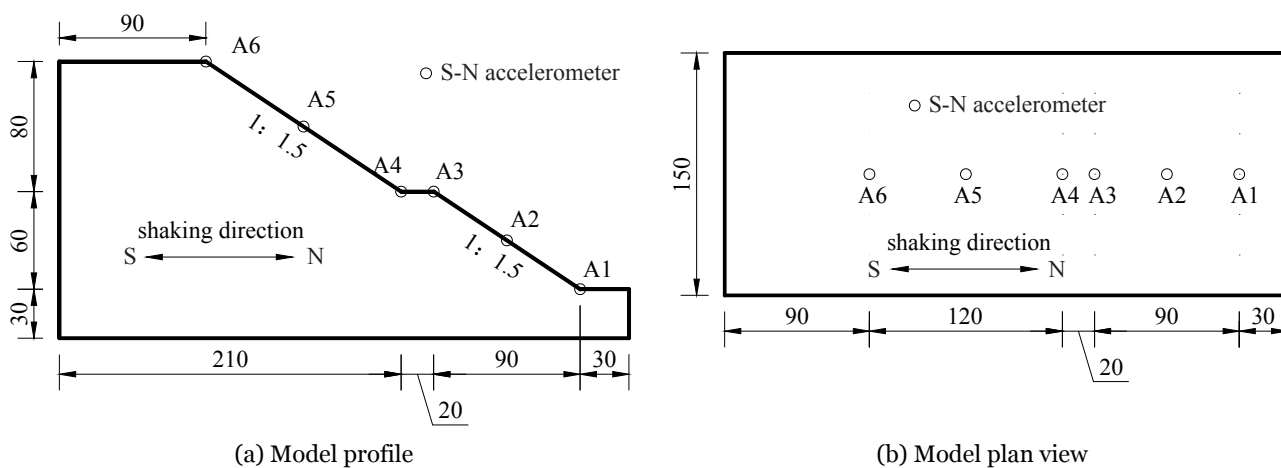


Figure 3 Layout of instrumentation with A1-A6 indicating the accelerometers (unit: cm)

prepared by mixing soil with water to reach 6.0% water content and then cured for 24 hours. The sample was compacted to a unit weight of 19.4 kN/m³ into the model box using the controlled-

volume method. The slope surface was compacted by a modeling tool to keep the slope angle at the designated value. The final slope sample is shown in Figure 3, with a height of 1.4 m, a width of 1.5 m,

and a slope of 1:1.5 (V:H). Direct shear tests were performed on the samples obtained from the model slope. The cohesion of the soil sample is nearly zero, and the friction angle is 42.3° .

In order to diminish the boundary effect, a shearing deformation model box was used, with a rubber membrane of 3 mm thickness lining the box. In order to simulate the prototype slope in the model test, the law of similitude was applied. In this study, the law of similitude was based on the factor considered to be the most important in the simulation. The main object in applying this law of similitude was keeping the soil density the same for both the prototype and the model, which would simplify the needs of scaling of parameters in the 1 g model testing. The corresponding scaling of parameters between the prototype and the model, shown in Table 1, from JIANG et al. 2009), is used in this experiment.

2.2 Seismic Input and Loading Rule

According to YAO (2009): “Field investigation showed that horizontal seismic force played a

dominant role in instability of subgrade engineering even in meizoseismal area for Ms8.0 Wenchuan earthquake.” We only consider horizontal ground acceleration in the study for reasonable simplification.

Strong ground motion adopted for the model tests was based on the Wolong (WL) record in the EW direction during the main shock, which was recorded on a bedrock site, 1.09 km north of fault rupture. The WL record in the EW direction during the main shock (PGA was 9.57 m/s^2) was determined from the two main accelerograms of 51.2 s to be the input acceleration (see Figure 4).

According to the traditional definition of earthquake ground motion duration, $\text{duration} = T_2 - T_1$, where T_1 is the time that acceleration first exceeds a $\text{PGA}/3$, and T_2 is the time that acceleration last exceeds a $\text{PGA}/3$ (see Figure 4).

WL was scaled to produce PGA’s of 0.85 m/s^2 , 3.12 m/s^2 and 6.16 m/s^2 , corresponding to different seismic intensities, and time was compressed according to the similitude coefficients and the loading sequence shown in Table 1 and Table 2, respectively.

Table 1 Primary similitude coefficients of model (JIANG et al. 2009)

Physical Quantity	Similarity Relationship	Similarity Constant		Remark
Length (m)	C_l	10	5	controlled variable
Density (kg/m^3)	C_ρ	1	1	controlled variable
Acceleration (g)	C_a	1	1	controlled variable
Friction angle ($^\circ$)	C_ϕ	1	1	
Time (s)	$C_t = C_\rho^{1/4} C_l^{3/4}$	5.62	3.34	
Frequency (Hz)	$C_\omega = C_\rho^{-1/4} C_l^{-3/4}$	0.18	0.30	

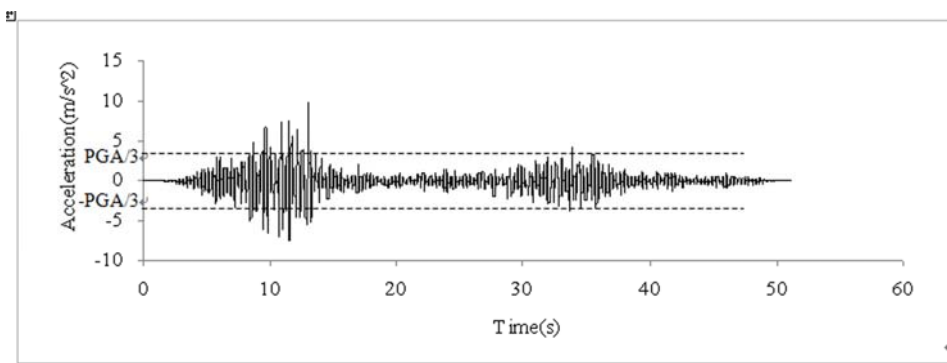


Figure 4 Earthquake record used in the model tests

Table 2 Loading sequence of shaking table test

sequence	mark	PGA(m/s ²)	Length scale (proto/model)	Time scale (proto/model)
1	WL1	0.85	10	5.62
2	WL2	0.85	5	3.34
3	WL3	0.85	1	1.00
4	WL4	3.12	10	5.62
5	WL5	3.12	5	3.34
6	WL6	3.12	1	1.00
7	WL7	6.16	10	5.62
8	WL8	6.16	5	3.34
9	WL9	6.16	1	1.00

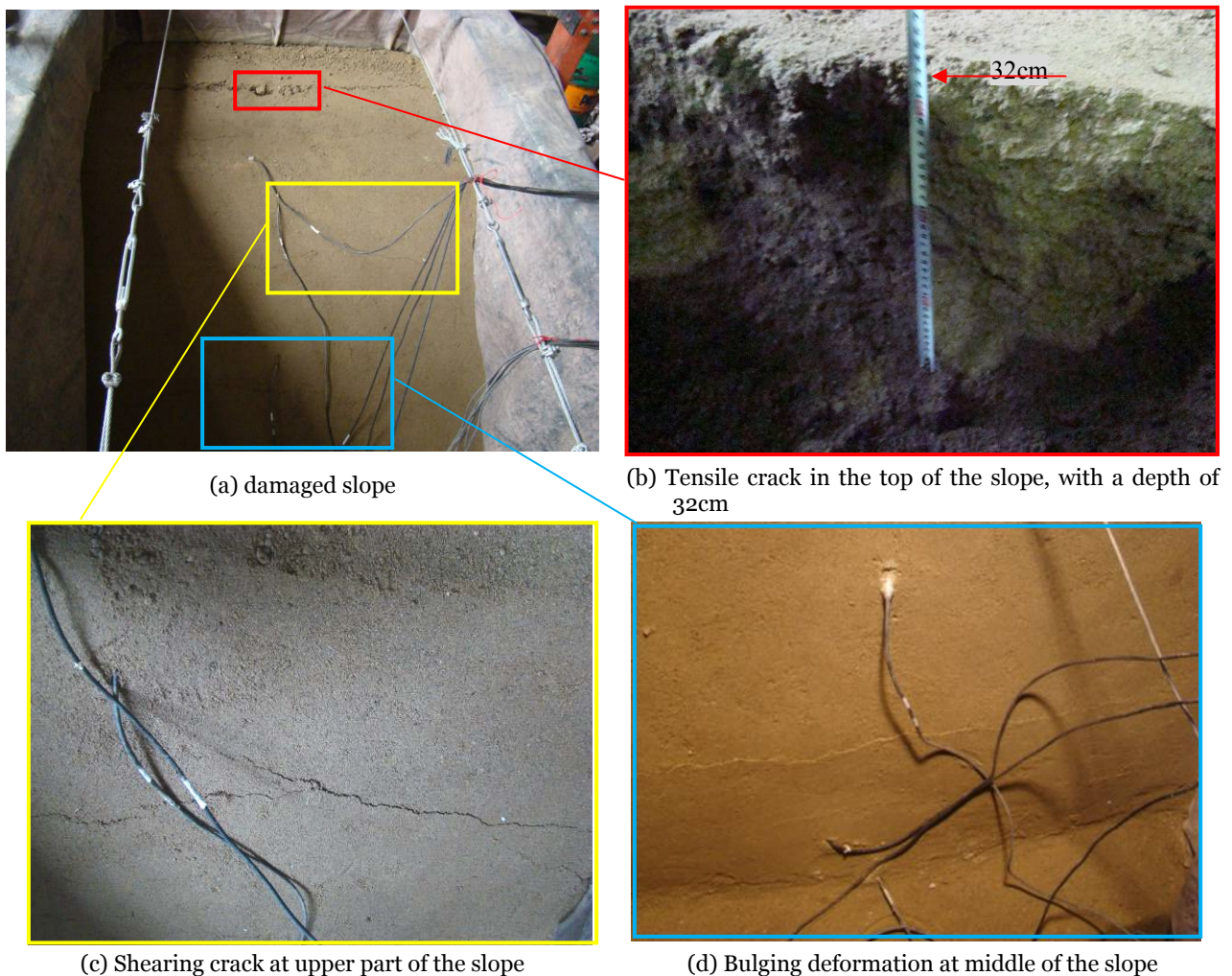


Figure 5 Failed model slope after the application of loading sequence of Table 2

2.3 Test Results and Discussion

A total of three model tests with the same shape, material and loading rule were conducted,

and the results corresponded very well. Results of one model slope are presented.

With the loading sequence in Table 2, the failed status of the model slope is shown in Figure

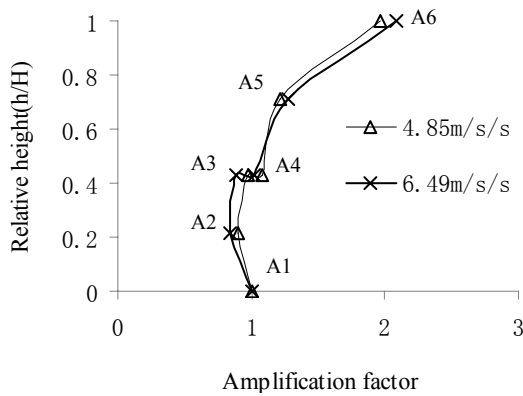


Figure 6 Amplification factor of PGA on slope surface by model tests

5a. A tension crack in formed in the top of the slope 50 cm away from the slope crest, with a steep surface of 32 cm (see Figure 5b), i.e., 3.2 m in the prototype slope with a height of 14 m when the length scale (proto/model) is 10(see Table 1). There were shear cracks in upper part (see Figure 5c) and bulging deformation in the middle of the slope (see Figure 5d), but the lower part of the slope was still intact. The upper part of the model slope was shattered by the earthquake, while the lower part was still intact. Results of the model tests coincided with the findings of the field investigation very well.

Analyzing measured accelerations (when the measured accelerations on shaking table are 4.85 m/s² and 6.49 m/s², see Figure 6), it is found that the amplification factor of Peak Ground Acceleration (PGA) on a slope surface rises with height on the whole, with a significant increase in the upper part of the slope (from position A5 to A6 in Figure 6). The maximum value of amplification factor is about 2 at the crest. Acceleration at the top of the slope is about twice the value of that at the toe, which means that seismic force at the top of

the slope is twice that at the toe.

3 Numerical Analysis of a Generalized Model

3.1 General Situation

To better understand the mechanism of the slope instability, a finite difference dynamic analysis of the soil slope was performed. A simplified model of typical slopes along the Dujiangyan-Yingxiu highway has a width of 10 m; a height of 20 m and a slope angle of 45° (see Figure 7). Free field is added around the model to diminish boundary effects. Seismic wave inputs are at the bottom of model, which is the same as shaking model test (see Figure 4).

ZHENG et al. (2009) proposed a dynamic-strength-reduction model to simulate the formation of the sliding surface of a soil slope, which reduced shear and tensile strength parameters as follows:

$$c' = \frac{c}{\omega}, \quad \phi' = \arctan\left(\frac{\tan\phi}{\omega}\right), \quad \sigma'_t = \frac{\sigma_t}{\omega} \quad (1)$$

where c , ϕ , σ_t and c' , ϕ' , σ'_t are cohesion, friction and tensile strength of the soil before and after reduction, separately, and ω is the factor of reduction. By use of this method and the reduction of shear and tense strength parameters of soil gradually until triggering a sliding surface, the character and location of the failure surface were analyzed.

For this analysis, an elastic-perfectly plastic constitutive model with Mohr–Coulomb failure criterion was adopted. Different from the model

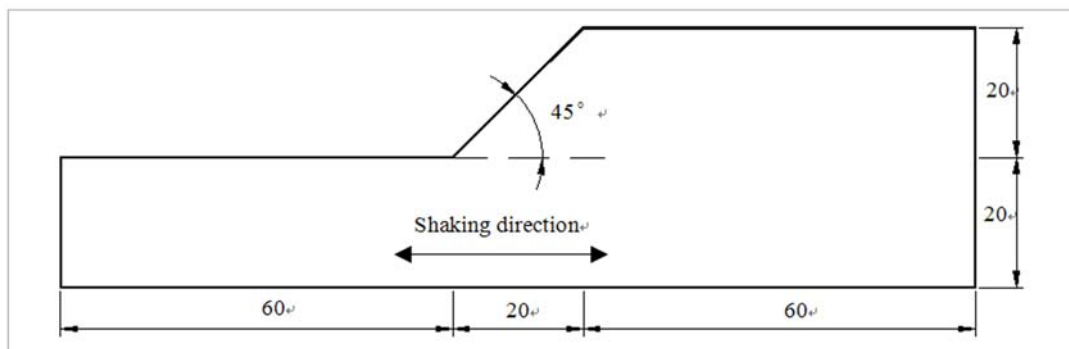


Figure 7 Geometrical configuration of the model used in the analysis (unit:m)

tests, which require sandy soil to find the failure patterns in a slope, more commonly clay soil was chosen in numerical analysis, with a unit weight of 20.0 kN/m³, which is distributed widely along the Dujiangyan-Yingxiu highway, as a complement to, and verification of, the results of shaking model tests. Besides, the effect of material on test results is reduced by use of the dynamic-strength-reduction method. The cohesion of the soil material is 40 kPa, and the friction angle is 20°. The shear modulus is 29.8 MPa and bulk modulus is 64.5 MPa. The damping in the numerical analysis is 15%. Based on the results of our field investigation, pore pressure generation due to earthquake loading was not incorporated in the model.

3.2 Analysis of Slope Distress Patterns under Dynamic Conditions

The factor to reduce (ω) was set to 1.2 here, so cohesion and friction angle were reduced to 33.3 kPa and 16.87° separately. Plastic status and shear strain increment of the zone were analyzed to discover the failure mechanism and sliding surface of a landslide under a seismic wave with a PGA of 10 m/s².

According to the nephograms of shear strain increment (see Figure 8a), the shear zone stretches upwards from the toe and stops at a distance of 5-6 m from the top of the slope. Even until the sliding of landslide, the shear zone cannot propagate to the top, because zones have already yielded to tension at the top of the slope with a depth of 5-6 m (see Figure 8b). The dynamic failure surface of the slope is made up of tension cracks in the upper part and a shear zone in the lower part commonly,

which is different from static failure surface of a shear zone only. Thus it can be taken that tension cracks shattered by an earthquake at the top of the slope are typical for landslides initiated by earthquakes.

3.3 Failure Surface of Slope under Earthquake

Based on these findings, it is suggested that the key point of anti-seismic design is to prevent tension cracks from forming in the upper portion of the slope, and that preventive treatment for secondary mountain hazards post-earthquake should mainly involve restraining the development of tension cracks. A simplified procedure for estimating the depth of earthquake-induced tension cracks will hopefully be developed.

Failure surfaces under the Wolong acceleration with different amplitudes (1-10 m/s²) were calculated with a reduction factor of 1.2.

Comparisons between a gravity-induced sliding surface, an earthquake-induced sliding surface and a sliding surface calculated by the pseudo-static method are shown in Figure 9. It was found that depth of an earthquake-induced sliding surface increases with the increase in intensity of seismic motion. Within 5 m from the top of slope, the dynamic sliding surface will be about 1 m shallower than the pseudo-static sliding surface in a horizontal direction when the PGA is 1 m/s², the dynamic sliding surface will be about 2 m deeper than the pseudo-static sliding surface in a horizontal direction when the PGA is 10 m/s², and the depths of a dynamic sliding surface and a pseudo-static sliding surface will be almost the same when the PGA is 2 m/s². It is found that a

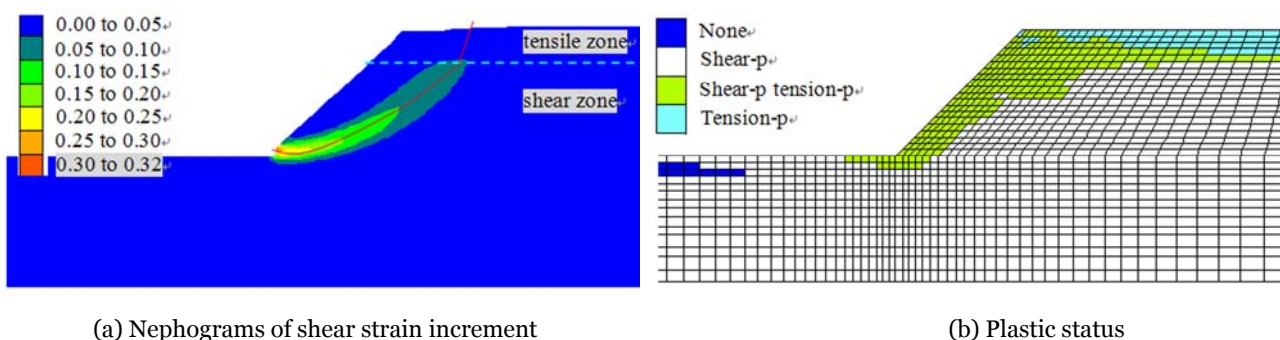


Figure 8 Failure status of slope under earthquake

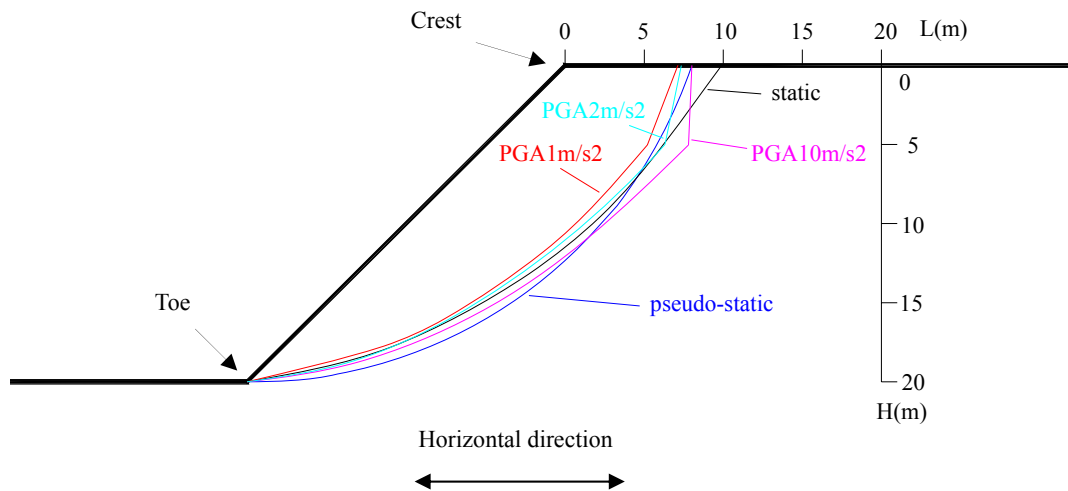


Figure 9 Slip surfaces from different analysis methods

dynamic sliding surface is always deeper than a static sliding surface.

4 Conclusions and Discussion

This paper inquires into earthquake-triggered failure modes, failure mechanisms and the failure surfaces of slopes by means of field investigation, shaking table model tests and numerical analysis. The major conclusions from these analyses can be summarized as follows:

(1) Slopes were shattered and damaged during the Wenchuan earthquake, and open tension cracks formed in the tops of the slopes. Upper parts of the slopes collapsed and slid, while lower parts of the slope remained intact, which indicated that the upper part of the slope would be damaged more heavily than the lower part during an earthquake.

(2) Large-scale shaking table model tests reproduced the process of deformation and failure of slopes. Tension cracks emerged at the top and upper parts of the modeled slopes, while the bottoms of the modeled slopes remained undamaged, which is consistent with the field investigation. Depth of the tension crack at the top of the model was 32 cm, i.e. 3.2 m compared to the prototype slope with a length scale (proto/model) of 10, and acceleration at the top of the slope was almost twice as large as that at the toe, which means that seismic force at the top of the slope is

twice the magnitude of that at the toe.

(3) By use of the dynamic-strength-reduction method, numerical simulation was conducted to explore the process and mechanism of formation of the sliding surface, and other quantified information. An earthquake-induced failure surface commonly is made up of tension cracks and a shear zone. Within 5 m from the top of slope, the dynamic sliding surface will be about 1 m shallower than the pseudo-static sliding surface in a horizontal direction when the peak ground acceleration (PGA) is 1 m/s², the dynamic sliding surface will be about 2 m deeper than the pseudo-static sliding surface in a horizontal direction when the PGA is 10 m/s², and the depths of the dynamic sliding surface and pseudo-static sliding surface will be almost the same when the PGA is 2 m/s².

(4) Because of the complexity of the geotechnical structure and of nonlinear dynamic behavior, the failure surface depth calculated exactly here is not only confined to the given conditions but can be a reference to other situations. As to important slopes, special studies should be conducted to get a more reasonable result based on the actual conditions.

5 Recommendations

Based on these findings, it is suggested that

the key point of anti-seismic design is to prevent tension cracks from forming in the upper part of the slope, and that preventive treatment of post-earthquake, secondary mountain hazards should be concentrated on restraining the development of tension cracks. Therefore, the depth of the tension cracks from the slope surface is the key to the reinforcement of slopes. The depth of the sliding surface determined by the pseudo-static method can be a reference for slope reinforcement.

References

- Baker, R., Shukha, R., Operstein, V., et al. 2006. Stability charts for pseudo-static slope stability analysis. *Soil Dynamics and Earthquake Engineering* 26(9):813-823.
- CHEN, T. C., LIN, M. L., HUNG, J. J. 2004. Pseudostatic analysis of Tsao-Ling rockslide caused by Chi-Chi earthquake. *Engineering Geology* 71(1):31-47.
- Crespellani, T., Madiac, Vannuchi, G. 1998. Earthquake destructiveness potential factor and slope stability. *Geotechnique* 48(3): 411-419.
- CUI Peng, CHEN Xiaoqing, ZHU Yingyan, et al. 2009a. The Wenchuan earthquake (May 12, 2008), Sichuan Province, China, and resulting geohazards. *Nat Hazards*. DOI: 10.1007/s11069-009-9392-1.
- CUI Peng, ZHU Yingyan, Han Yongshun, et al. 2009b. The 12 May Wenchuan Earthquake-induced Landslide.
- Havenith, H. B., Vanini, M., Jongmans, D. 2003. Initiation of earthquake-induced slope failure: influence of topographical and other site specific amplification effects. *Journal of Seismology* 7(3): 397-412.
- HUANG Runqiu. 2009. Mechanism and geomechanical modes of landslide hazards triggered by Wenchuan 8.0 earthquakes. *Chinese Journal of Rock Mechanics and Engineering* 28(6):1239-1248. (In Chinese)
- JIANG Liangwei, YAO Lingkan, WANG Jian. 2009. Similitude for shaking table model test on side slope relating to dynamic characteristics and strength 25(2): 1-7. (In Chinese)
- Jibson, R.W. and Keefer, D.K., 1988. Landslides Triggered by Earthquakes in the Central Mississippi Valley, Tennessee and Kentucky, U.S. Geological Survey Professional Paper 1336-c.
- Jibson, R.W., Keefer, D.K. 1993. Analysis of the seismic origin of landslides: examples from New Madrid seismic zone, *Bulletin of Geological Society of America*, Vol. 105. Pp. 521-536.
- LI Xinpo, HE Siming. 2009. Seismically induced slope instabilities and the corresponding treatments: the case of a road in the Wenchuan earthquake hit region. *Journal of Mountain Science* 6(1):96-100.
- LIN Meiling, WANG Guolong. 2006. Seismic slope behavior in a large-scale shaking table model test. *Engineering Geology* 86(2):118-133.
- WANG Genlong, ZHANG Junhui, LIU Hongshuai. 2009. Investigation and preliminary analysis of geologic disasters in Beichuan county induced by Wenchuan earthquake. *The Chinese Journal of Geological Hazard and Control* 20(3):47-51. (In Chinese)
- WANG Fawu, CHENG Qiangong, LYNN H., et al. 2009. Preliminary investigation of some large landslides triggered by Wenchuan earthquake in 2008, Sichuan Province, China. *Landslides* 6(1):47-54.
- Wilson, R. C., and Keefer, D. K. 1985. Prediction areal limits of earthquake-induced landslide, in Ziony, J. I., ed., *Evaluating earthquake hazards in the Los Angeles region-An earth-science perspective*: U.S. Geological Survey Professional Paper 1360. Pp. 316-345.
- Wright, S. G., Rathje, E. M. 2004. Triggering mechanisms of slope instability and their relationship to earthquakes and tsunamis. *Pure and Applied Geophysics* 160(11):1865-1877.
- YAO Lingkan, CHEN Qiang. 2009. New research subjects on earthquake resistant techniques of line engineering extracted from "5.12" Wenchuan earthquake. *Journal of Sichuan University (engineering science edition)* 41(3):43-50. (In Chinese)
- Youd, T.L. 1980. Ground Failure Displacement and Earthquake Damage to Buildings: American Society of Civil Engineers, Proceedings of the Specialty Conference on Civil Engineering and Nuclear Power, Vol. 2. Pp. 7-6-1-7-6-26.
- ZHENG Yingren, YE Hailin, HUANG Runqiu. 2009. Analysis and discussion of failure mechanism and fracture surface of slope under earthquake. *Chinese Journal of Rock Mechanics and Engineering* 28(8):1714-1723. (In Chinese)

Acknowledgements

This work was supported by 973 Program, Grant No. 2008CB425802, National Natural Science Foundation of China and supported by the Fundamental Research Funds for the Central Universities (SWJTU09ZT04). The comments of the reviewers and help provided by the Guest Editors improved the quality of the paper and are deeply appreciated by the authors.